

Scanning tunneling microscopy of Ir adsorbed on a Ge(111) surface

Dylan Lovinger
University of Massachusetts Amherst

August 28, 2011

Abstract. The surface structure and growth characteristics of Ir adsorbed on a clean Ge(111) surface was examined using Scanning Tunnelling Microscopy (STM). At an adsorbent coverage of approximately 0.5 monolayers (ML) the sample is annealed in the temperature range $640\text{K} < T < 700\text{K}$. In this temperature regime, STM images reveal the formation of Ir islands and smaller connecting pathways at atomic or near-atomic resolution. We focus our study on the emergence of these Ir pathways and the mechanism of their formation by annealing at 15K intervals and subsequently imaging. Emergence of the pathways is found to be in the range $640\text{K} < T < 655\text{K}$, while disappearance is in the $700\text{K} < T < 715\text{K}$ range.

1. Introduction

The data presented here has been collected at the UC Davis Advanced Surface Microscopy Facility, where recent efforts have focused on studying the growth of metals on semiconductors. An understanding of the semiconductor surface and how it reacts and reconstructs in the presence of an adsorbent is extremely relevant to the field of electronics, as well as other materials sciences. In particular, we have focused our efforts on observing the growth of Ir on Ge(111). This Ir-Ge interface remains understudied relative to, for example, the more extensively studied Pt-Ge, Au-Ge and Ag-Ge interfaces [2-6]. Our analysis reveals a growth mechanism seemingly unique to Ir on Ge(111) in the temperature range $640\text{K} < T < 700\text{K}$, where narrow Ir pathways emerge between Ir islands. These pathways are also observed along Ge step edges, and connecting step edges to islands. We will describe the relevant background information and experimental setup, and then present and discuss the data collected.

Bulk germanium has a diamond cubic crystal structure, a face centered cubic lattice with four additional atoms tetrahedrally bonded (Figure 1). The sample studied here is Ge(111), the parenthetical addendum referring to the orientation of the surface. The wafer is cut along a plane normal to a vector in the 1,1,1 direction, where the origin sits at the corner of the cubic unit cell. The surface structure of Ge, and any solid, differs distinctly from that of the bulk however. The lack of an additional layer of atoms changes the energy profile at the surface, and these atoms rearrange themselves to minimize their potential energy. By annealing a clean sample we allow surface atoms to overcome local minima, further minimizing energy, and achieve an organized structure. In Ge(111) the reconstructed surface has been well studied and is known to take on a $c(2 \times 8)$ structure [7], a rotated unit cell centered at an adatom (Figure 2). Likewise, the addition of an adsorbant may result in further surface reconstruction after annealing.

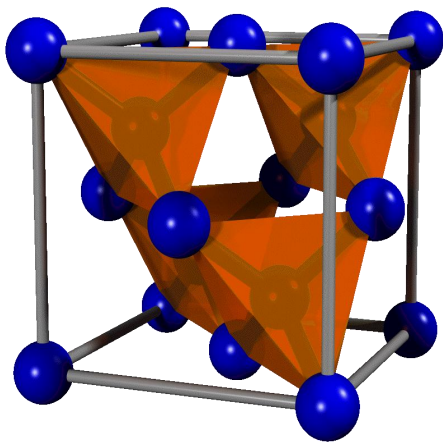


Figure 1: The diamond cubic unit cell of germanium. Note the tetrahedral structures in orange. [Wikimedia]

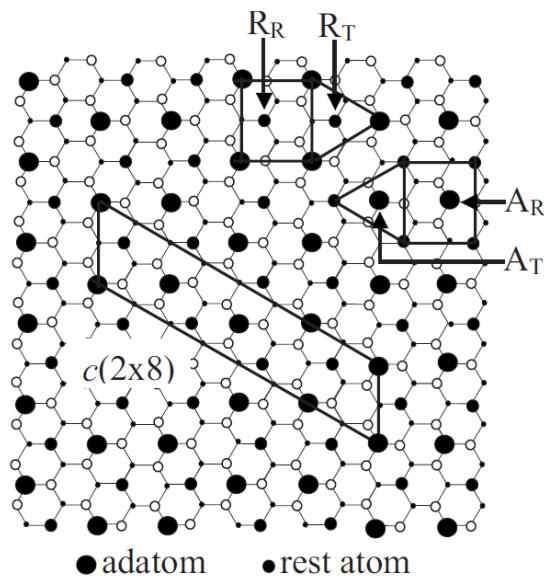


Figure 2: The $c(2 \times 8)$ surface reconstruction after annealing. The unit cell is 2 lattice sites tall and 8 wide, slanted. The total hexagonal lattice consisting of the 1st and 2nd layer of atoms is also visible. [7]

2. Experiment: Apparatus and Procedure

The facility at UC Davis includes equipment for Low-Energy Electron Microscopy (LEEM), X-Ray Photoelectron Spectroscopy (XPS) and Scanning Tunnelling Microscopy (STM), all within a single Ultra-High Vacuum (UHV) setup [8] (Figure 3). Transfer bars and manipulators allow movement of the sample to and from the chambers and instruments without breaking UHV. The sample holder itself is specifically designed for compatibility with both the LEEM and STM, and includes a thermocouple and heating filament for precision annealing. In addition to the XPS instrument, the analysis chamber houses an Ar-ion sputtering gun used for cleaning samples.

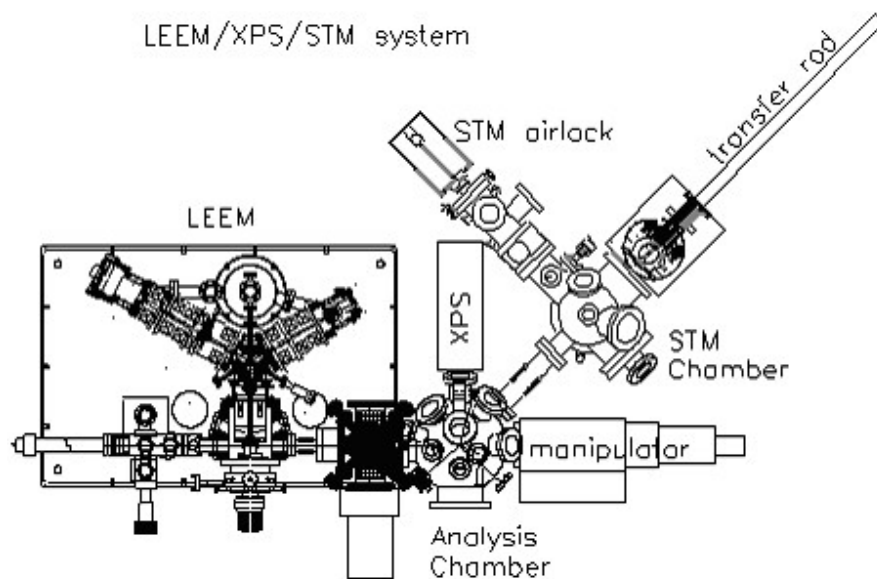


Figure 3: Schematic of the LEEM/XPS/STM system at UC Davis. The full setup is operated in UHV, at $\sim 10^{-10}$ Torr. [8]

The data presented here was collected using only STM. This microscopy method allows atomic resolution imaging of metals and semiconductors by exploiting a quantum tunnelling effect. An atomically sharp tungsten wire tip is placed a few Angstroms from the sample and a small potential applied between the two. Electrons from the electron cloud in the sample ‘tunnel’ through the vacuum toward the tip (or from tip to sample, if using a negative tip bias) to produce a tunnelling current (Figure 4). The majority of our data uses a positive tip bias of +2V. This current drops exponentially with distance, and as such the current is extremely sensitive to the height of the local electron cloud and thus to the positioning of surface atoms. The tunnelling current I is given by the relationship

$$I = Ve^{-A\sqrt{\phi}z}$$

where V is the applied voltage, A is a normalizing constant, ϕ the average work function of tip and sample, and z the distance between tip and sample [9,10]. By sweeping the tip back and forth across the surface, an image can be constructed from the current profile with a vertical resolution of 0.01 Angstroms and a lateral resolution of 2 Angstroms. Though a very fine tip is required for true atomic resolution, the distinction between adsorbant and substrate is nearly always distinct, as well as step edges and other surface structures.

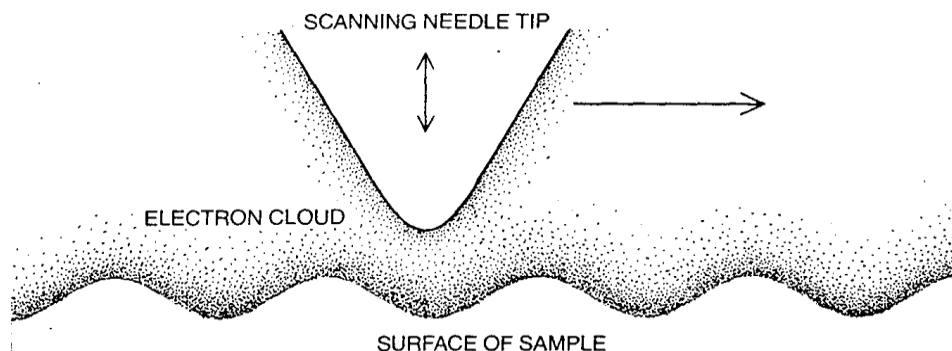


Figure 4: *STM operation. The motion of this tip represents one lateral sweep. A full image is composed of 512 of these sweeps.*

Before imaging a sample, the Ge(111) wafer must be properly cleaned. We use a SPECS Argon-ion sputtering gun to clean the sample, at a beam energy of 0.25 KeV and Ar pressure of $1.3E-5$ torr for 15 minutes (a second power supply was later used, at 0.40 KeV beam energy, 15.0 mA emission current and Ar pressure of $5.5E-5$ torr). The sample is then annealed at $\sim 815K$ for 10 minutes. This sputter/anneal process is repeated 16 times for a new sample, with a final anneal for 30-45 minutes. The clean sample is then dosed with Ir for 8 minutes using an e-beam evaporator, where electrons produced by a hot filament bombard and heat an Ir block. We use a filament current of 4.20A and a voltage difference of 4000V between the filament and Ir block, and record an electron beam current of $\sim 48mA$. The Ir e-beam doser was calibrated at these parameters using LEEM, where 16 minutes of dosing corresponds to 1ML coverage. Our 8 minutes of dosing then corresponds to ~ 0.50 ML of Ir. The sample is annealed a final time at a precise temperature for 5 minutes to allow nucleation of the adsorbed Ir. It is allowed to cool to room temperature for 3 hours before imaging with STM. Data is taken at 640K, 655K, 670K, 685K and 700K anneals, with 5 sputter/anneal cleanings and redosing between.

3. Results and Discussion

Figure 5 depicts the characteristic surface structure of Ir on Ge(111) in the temperature range $640\text{K} < T < 700\text{K}$. Image B) scaled to 66% to account for the smaller scale of the original image. The light circular formations in each image are Ir islands and the often irregular bright spots are tall Ir peaks. The remaining space is the germanium surface. Image A) shows a large number of

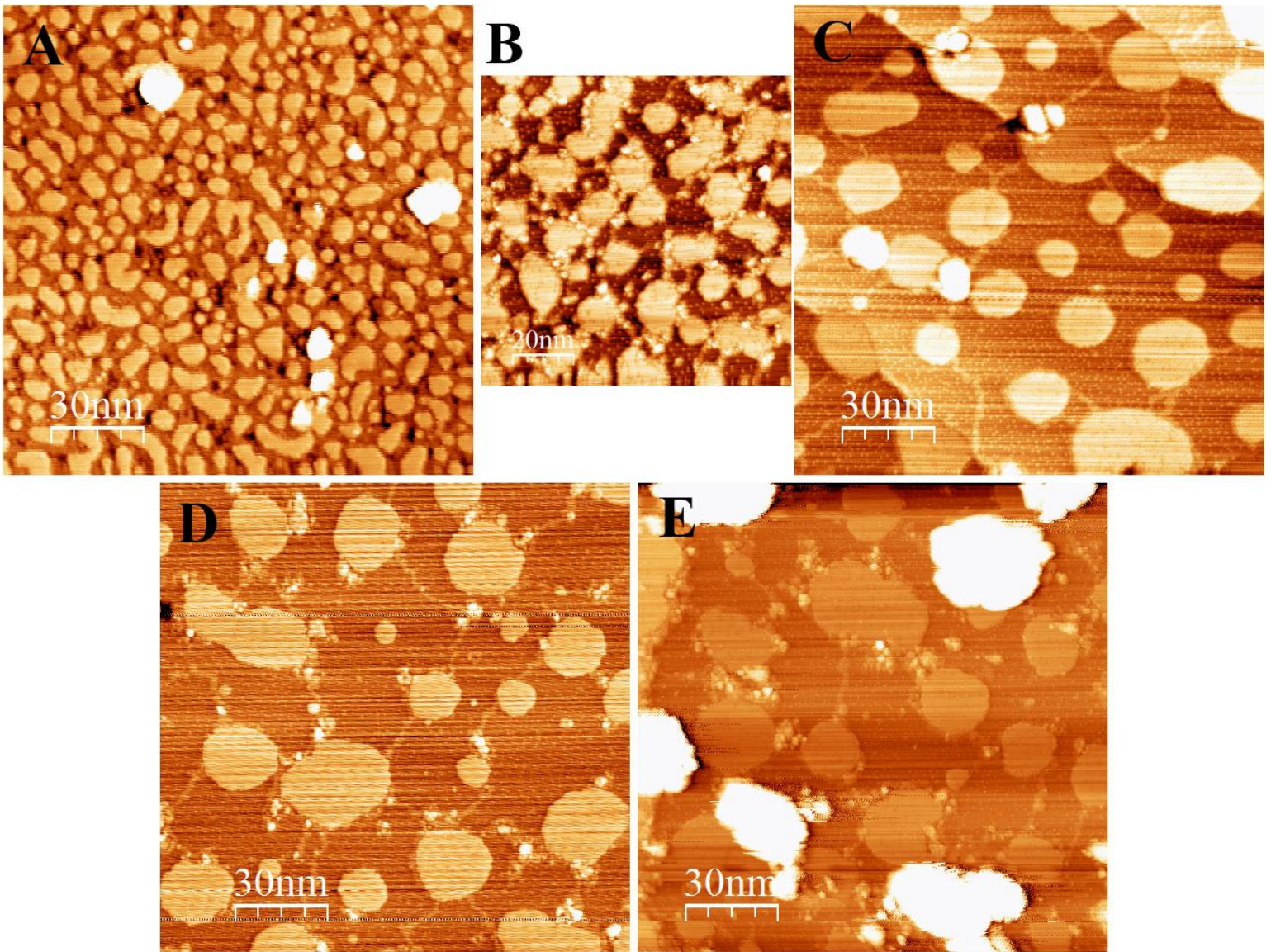


Figure 5: Ir on Ge(111) annealed at A) 640K, B) 655K, C) 670K, D) 685K and E) 700K. Light regions are Ir islands, while the darker regions are the Ge(111) surface. Image B) is scaled to 66%, as it was taken at smaller resolution. Note the progression in Ir island size and the emergence of pathways near 655K. The relative width of the Ir pathways decreases from 670K to 700K.

small Ir islands, many merging to form larger islands by Ostwald ripening. In image B) the islands are visibly larger, and pathways begin to emerge between them. It seems possible that the Ir coverage in images A and B is slightly greater than 0.5 ML. In each remaining image Ir pathways are clearly visible between islands, and even connecting islands to step edges. In image C) note the pathway affinity for step edges. It appears that when a step edge is nearby the pathways will prefer to grow along the edge. In none of the images taken are pathways visibly isolated from larger Ir structures.

It is important to note the progression of island and pathway size as the sample is annealed at higher temperatures. The temperature range $640\text{K} < T < 670\text{K}$ appears to be a defining zone in island formation, where islands clump together to grow much larger and less numerous with increasing annealing temperature. Beyond 670K the islands remain a constant size. The range $640\text{K} < T < 670\text{K}$ is also the defining region for pathway emergence and evolution, with paths first appearing between 640K and 655K. Between 655K and 670K the pathways grow much longer as islands continue to spread and grow by Ostwald ripening. Beyond 670K the pathways begin to dramatically decrease in size and grow more irregular. Additional data in smaller annealing intervals between 640K and 655K is needed to pinpoint the region of pathway emergence. Further data between 655K and 670K is also needed to determine when the islands cease growing.

Figure 6 is Ir on Ge(111) annealed at 640K, very similar to fig. 5 A). Again note that the Ir coverage may be greater than $\frac{1}{2}$ ML. Figure 6 B) shows a different region than that in image A), and at a higher magnification. From both images it is clear that Ir pathways have not yet begun to form. Image B) clearly show islands of many different shapes and sizes, some merging together.

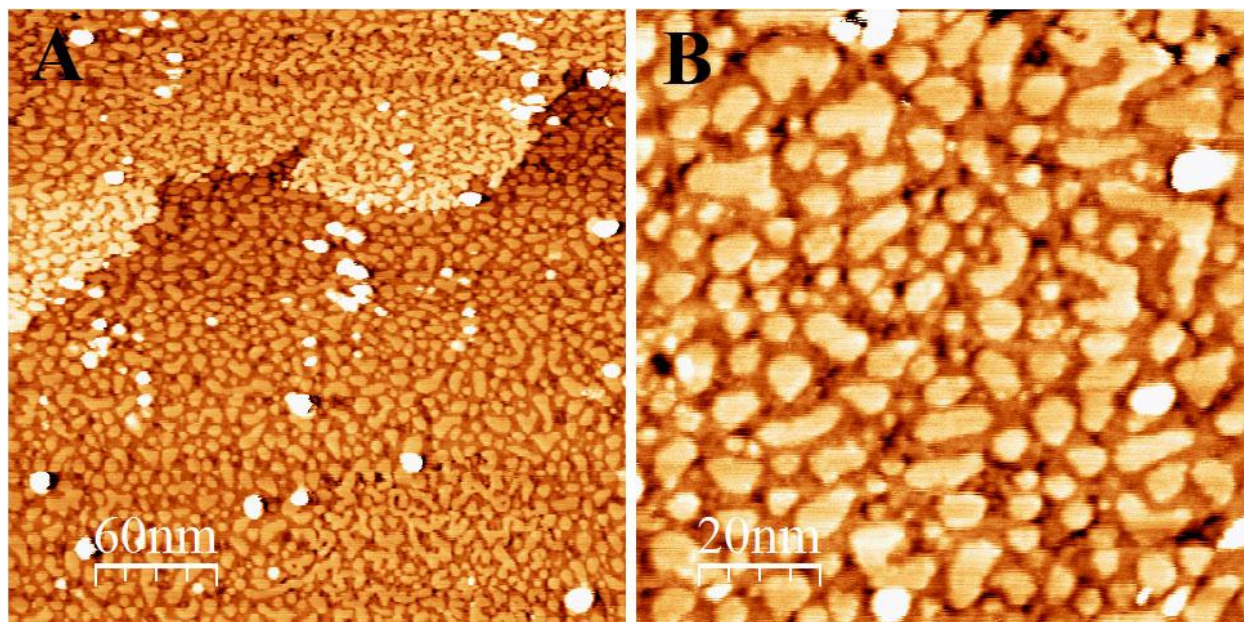


Figure 6: Ir on Ge(111) annealed at 640K for 5 minutes. A Ge step edge is visible in image A, in the upper region. Image B is a different region at triple magnification. The Ir islands are small and numerous.

Figure 7 is the data taken at an annealing temperature of 655K. Islands are much larger than at 640K, beginning to take on a more defined shape. Pathways are in the beginning stages of formation, and may be emerging as islands pull away from each other and merge with others. The resolution is also sufficient to discern isolated Ir adatoms on the Ge surface, seen as the small bright dots randomly scattered across the darker background. Similar structures are also visible within the pathways themselves, as can be seen in image B). Image C) is a height profile across the pathway and across an isolated adatom in image B). The peaks occurring for position x between 2-3nm are ‘bumps’ on the pathway and the peak at 5nm is the isolated adatom. If the pathways are not composed of these same adatoms, or atomic-sized Ir islands, they certainly have a vertical displacement similar to that of individual adatoms. More data, especially at a higher resolution, are needed to truly discern the atomic structure of the pathways.

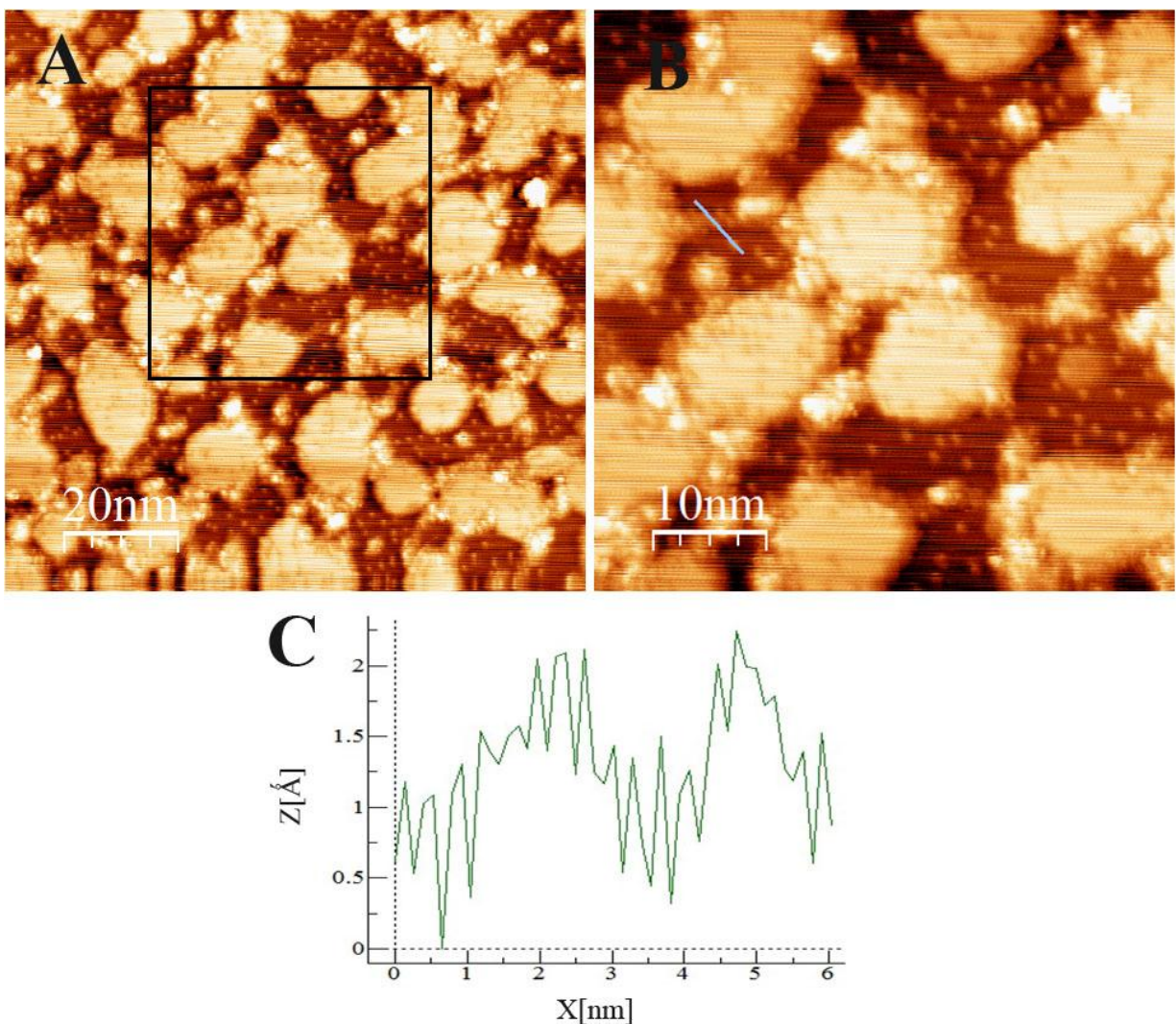


Figure 7: A), B) *Ir on Ge(111) annealed at 655K. B) is a detail of the boxed area in A. Individual adatoms are visible on the Ge surface, as well as on pathways. C) is a height profile of a pathway, across the blue line in B. The adatoms on the pathway lie at the same height as those on the Ge surface.*

Figure 8 shows relatively high resolution data at an annealing temperature of 670K. Image A) is a Ge step edge with a $\frac{1}{2}$ ML of Ir taken at a positive tip bias. Islands have taken on a definite circular shape and have stopped merging. Pathways are distinct and occur between nearly all islands, but also occur between islands and the base of the step edge. As also seen in fig. 5 C), pathways occur along the step edges themselves, preferring the edge over other regions. Isolated Ir adatoms distinctly appear as the scattered bright spots, and at a much higher density than those in fig. 7 (655k). Image B) is the same region as that in image A, but taken with a negative tip bias (the tip is now at -2V and the sample at 0V). The STM records electronic structure, such that changing the direction of electron current may change the image produced, as seen in B). The islands appear dimmer at this bias and pathways are less distinct, becoming thinner and more spindly. Additionally, the adatoms lying on the Ge surface almost entirely disappear. Since the image of a strictly metal surface should remain unchanged by a bias reversal, the evidence sug-

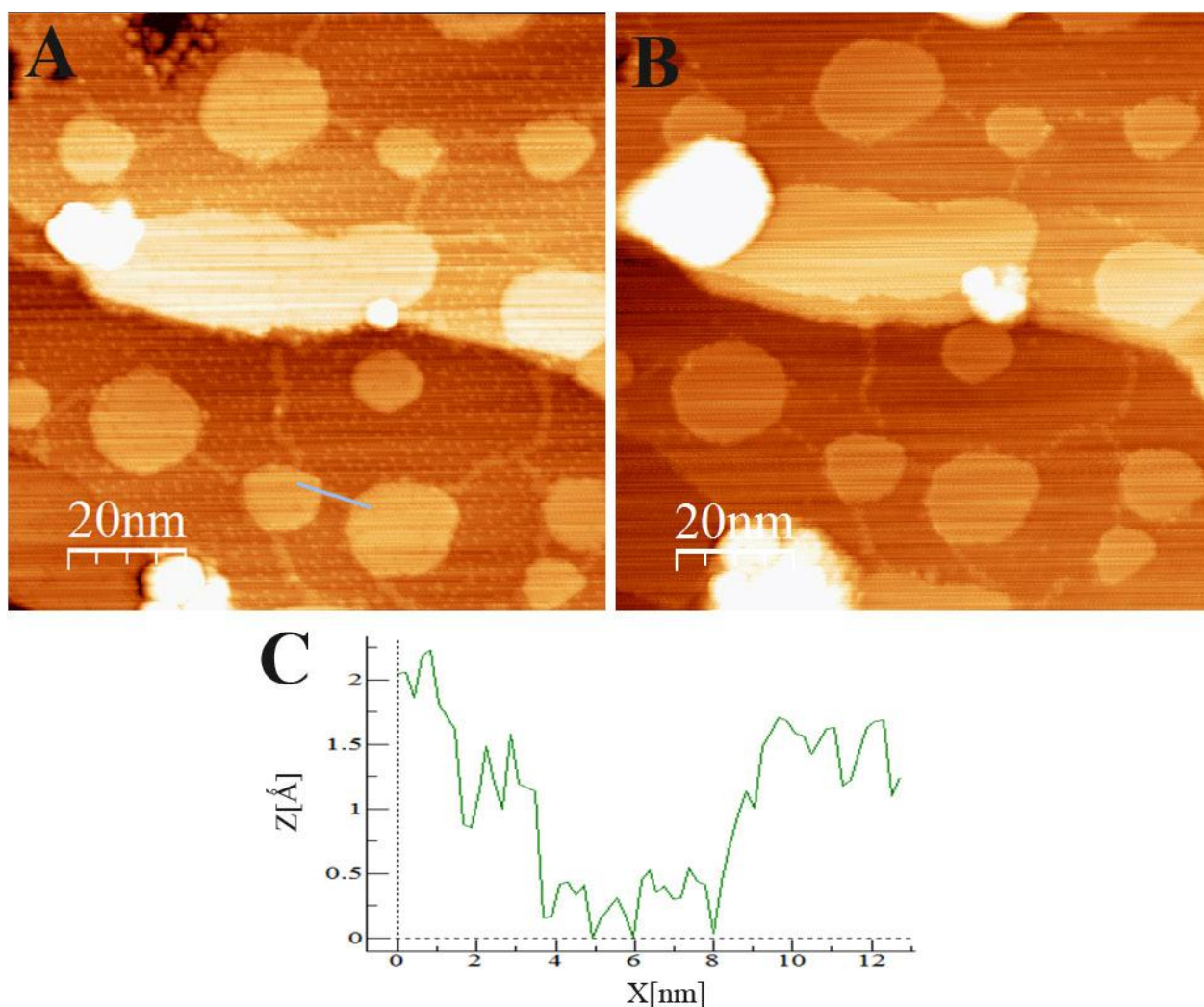


Figure 8: Ir on Ge(111) annealed at 670K. A) is a representative region, showing Ir islands, pathways and adatoms (smaller bright dots). B) is region A imaged with a negative tip bias; adatoms disappear and pathways are less distinct. C) is a height profile across a pathway in image A (blue line). The pathways occur at a lower height than the

gests that the entire surface, including the Ir formations, shows some characteristics of a semiconductor. Since Ir is a pure metal, figure 8 suggests that the Ir islands, pathways and adatoms may be a combined state of Ge/Ir, rather than pure Ir. Because our images with a positive tip bias appear brighter than those with a negative tip bias the sample is likely n-type, with extra electrons available to make a band gap jump. Initial I/V curves suggest semiconductor properties on the “Ir” islands as well, but more data are needed for confirmation.

Fig. 8 C) is a simple height profile along a pathway connecting two Ir islands, indicated by the blue line in image A. The pathway itself, occurring for x between 4-8nm, clearly lies on a level lower than the islands. The height jumps in the profile along the pathway may be individual atoms, but are more likely a recording of the streaks across the image.

Figure 9 shows two images taken at an annealing temperature of 685K. Both image A) and B) simply depict the decrease in Ir pathway size. The pathways also grow more irregular in shape relative to lower annealing temperatures. In image B) there appears to be a pathway along the large step edge, but it is irregular and much less defined than those along the edges in fig 8. A) and fig. 5 B) (670K). Ir adatoms are again present, especially in image B), but appear to be at a very slightly lower density than those found at 670K.

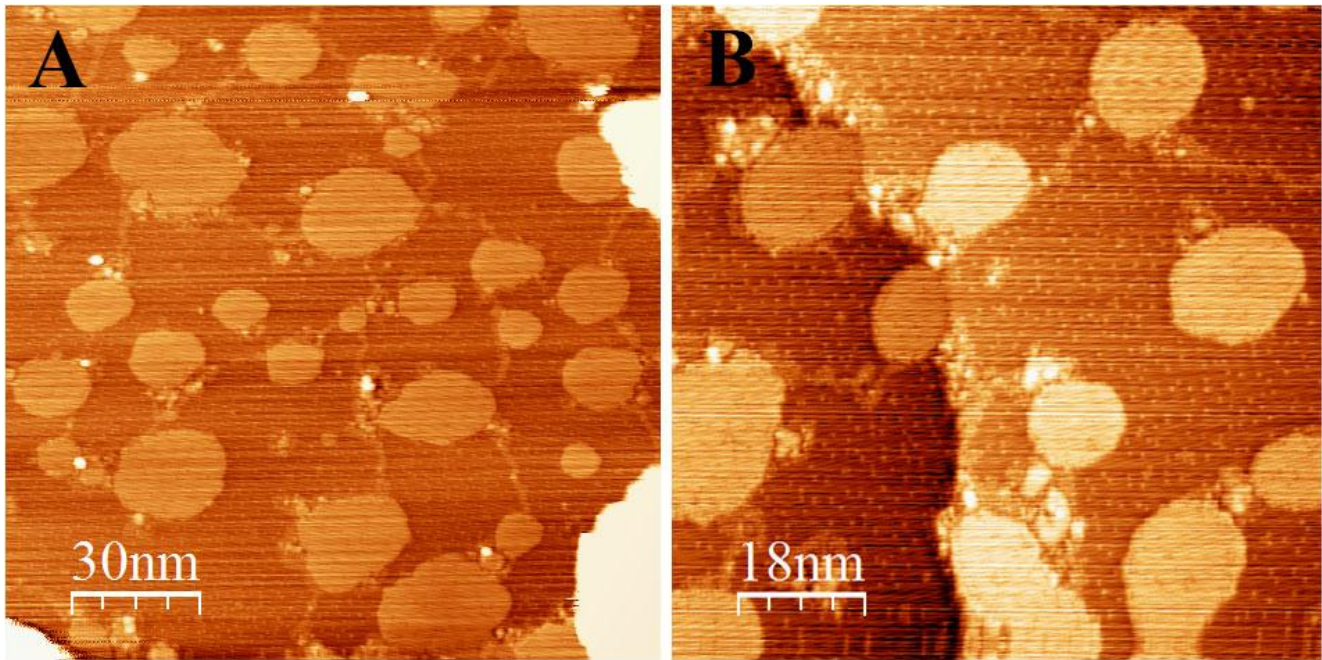


Figure 9: *Ir on Ge(111) annealed at 685K. A) and B) are representative images of the Ir structure at this temperature, with B) a smaller scale image. Note that the pathways are smaller and more irregular at this higher annealing temperature.*

Figure 10 shows data at an annealing temperature of 700K. Although it is a low quality image, Ir pathways are still visible. They are highly irregular and very small. Isolated Ir adatoms are not visible due to the poor resolution, but we would expect to find them in a lower concentration than at 685K.

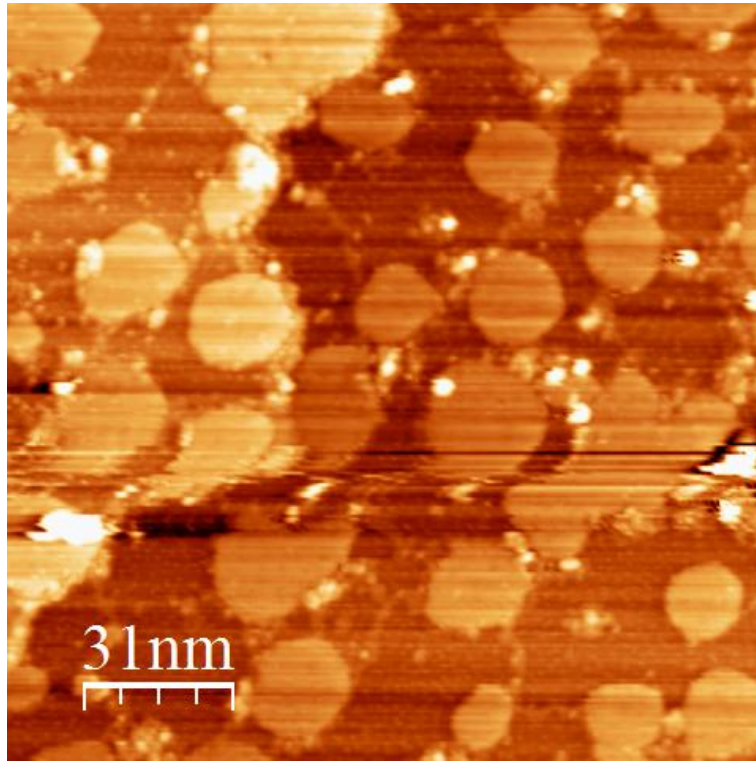


Figure 10: *Ir on Ge(111) annealed at 700K. Resolution is low, but Ir pathways can still be observed as small and highly irregular.*

4. Conclusion

Although there are insufficient data to make truly conclusive statements, we have strong preliminary results and a clear direction for future study. We observe a trend in Ir island density and size in the temperature regime studied ($640\text{K} < T < 700\text{K}$), and there is a clear progression in Ir pathway size as annealing temperature rises. There are not, however, sufficient data to make a statement on the relative number of pathways at different annealing temperatures. From the data collected, we conclude that Ir islands aggregate and grow until achieving a relatively stable size and shape between 655K and 670K. New data should be taken at 5K intervals in this range to more closely examine island maturation. Since Ir pathway emergence occurs just below or at 655K, new image sets should be taken at 650K and 660K to observe pathway formation. The data also suggest a maximum in Ir pathway size in a range near 670K, and data should be taken at 5K intervals around 670K to confirm this. Finally, data should be taken at 715K or higher to check for the suspected pathway disappearance in that temperature range. We have also observed a pathway affinity for step edges, suggesting that the edge is a lower energy region than open space.

Similar to the trend in Ir island and pathway size, there appears to be a trend in isolated Ir adatom concentration. It must be noted that there are much less data supporting this phenomenon than for island and pathway size progression. This trend follows the same temperature pattern as above, with individual Ir adatoms at highest concentration when the pathways are largest, near 670K. Figure 7 A) (655K) and figure 9 B) (685K) show lower concentrations below and above this temperature, respectively, though the concentration drop is much more significant at 655K. Higher resolution images and more data are needed to confirm or deny this trend.

Analyses of the data, especially at 655K and 670K, suggest that pathways lie at a height similar to that of the isolated adatoms on the Ge surface and at a height lower than the Ir islands. Higher resolution images suggest that the Ir pathways are composed of a nucleation of these isolated adatoms. Additional higher quality images are needed to determine the exact atomic makeup of the pathways, as well as their phase and structure.

Our data also suggest that what have been referred to as Ir islands, pathways and adatoms throughout this paper may not be pure Ir, but rather some mixture of Ir and Ge. For a negative tip bias, images appear darker, 'Ir' pathways are much thinner, and isolated adatoms disappear. Such evidence indicates that the full surface is behaving as a semiconductor, not just the Ge(111) substrate. That the images appear darker suggests it is an n-type semiconductor. Relatively little data has been taken to explore this, and important future work will include taking many more negative tip bias images, as well as extensive I/V curve studies. We predict that the 'Ir' formations will have a 'more metallic' I/V curve, which would consist of a mostly straight line, but curving near the voltage extremes. The background is expected to have a 'mostly semiconductor' I/V curve, with a steep jump in current at some voltage. Bright 'Ir' towers are expected to be pure Ir, and thus a straight I/V line. Atomic models are needed to compare with higher resolution images to confirm any of these hypotheses.

6. Acknowledgements

I would like to thank Dr. Shirley Chiang for her support, direction and excellent hospitality; Marshall Van Zijl for his willingness to help and extensive guidance in the LEEM lab, from training on the equipment to support with data and any other complications; William Mann and Dan Rubin for assistance with the Ir/Ge(111) project; Manuel Calderon de la Barca for organizing the REU program and activities therein; and the NSF for funding the UC Davis physics REU program.

References

- [1] O. Gurlu, H.J.W. Zandvliet, B. Poelsema, "Initial stages of Pt growth on Ge(001) studied by scanning tunneling microscopy and density functional theory," *Physical Review B*, 70, 085312, (2004).
- [2] L. Seehofer, R.L. Johnson, "STM study of gold on Ge(111)," *Surface Science*, 318, 21-28, (1994).
- [3] M. Gothelid, M. Hammar, M. Bjorkqvist, U.O. Karlsson, S.A. Flodstrom, "Geometry of the Ge(111)-Au($\sqrt{3}\times\sqrt{3}$)R30° reconstruction," *Physical Review B*, 50, 7, 4470-4475, (1994).
- [4] B.J. Knapp, J.C. Hansen, M.K. Wagner, W.D. Clendening, J.G. Tobin, "Occupied electronic structure of Au and Ag on Ge(111)," *Physical Review B*, 40, 5, 2814-2824, (1989).
- [5] M. Hammar, M. Gothelid, U.O. Karlsson, S.A. Flodstrom, "Initial growth of silver on Ge(111) studied by scanning tunneling microscopy," *Physical Review B*, 47, 23, 15669-74, (1993).
- [6] D.J. Spence, S.P. Tear, "STM studies of submonolayer coverages of Ag on Ge(111)," *Surface Science*, 398, 91-104, (1998).
- [7] I. Razado, J. He, H. Zhang, G. Hansson, R. Uhrberg, "Electronic structure of Ge(111)c(2x8): STM, angle-resolved photoemission, and theory," *Physical Review B*, 79, 20, 205410, (2009).
- [8] C.L.H. Devlin, D.N. Futaba, A. Loui, J.D. Shine, S. Chiang, "A Unique Facility for Surface Microscopy," *Materials Science & Engineering B*96, 215-220, (2002).
- [9] G. Binnig, H. Rohrer, "Scanning Tunneling Microscopy," *Helvetica Physica Acta*, vol. 55, 726735 (1982).
- [10] G. Binnig, H. Rohrer, "The Scanning Tunneling Microscope," *Scientific American*, 235, 50, (1985).